

# Excited electronic states from a variational approach based on symmetry-projected Hartree–Fock configurations

Carlos A. Jiménez-Hoyos,<sup>1</sup> R. Rodríguez-Guzmán,<sup>1,2</sup> and Gustavo E. Scuseria<sup>1,2</sup>

<sup>1</sup>*Department of Chemistry, Rice University, Houston, TX 77005*

<sup>2</sup>*Department of Physics and Astronomy, Rice University, Houston, TX 77005*

(Dated: February 27, 2024)

## Abstract

Recent work from our research group has demonstrated that symmetry-projected Hartree–Fock (HF) methods provide a compact representation of molecular ground state wavefunctions based on a superposition of non-orthogonal Slater determinants. The symmetry-projected ansatz can account for static correlations in a computationally efficient way. Here we present a variational extension of this methodology applicable to excited states of the same symmetry as the ground state. Benchmark calculations on the  $C_2$  dimer with a modest basis set, which allows comparison with full configuration interaction results, indicate that this extension provides a high quality description of the low-lying spectrum for the entire dissociation profile. We apply the same methodology to obtain the full low-lying vertical excitation spectrum of formaldehyde, in good agreement with available theoretical and experimental data, as well as to a challenging model  $C_{2v}$  insertion pathway for  $BeH_2$ . The variational excited state methodology developed in this work has two remarkable traits: it is fully black-box and will be applicable to fairly large systems thanks to its mean-field computational cost.

## I. INTRODUCTION

The quantum mechanical character of a chemical system is reflected in the discrete spectrum of electronic excitations. From the theoretical point of view, the prediction of geometries and excitation energies provides a means to interpret experimental electronic spectra. In addition, optically forbidden states, which often play an important role in the radiationless relaxation of a molecule, can be accessed.

When the excited state of interest has a different symmetry than the ground state, one can use a ground-state formalism. In the Hartree–Fock (HF) approximation, this approach is usually referred to as the  $\Delta$ -SCF (self-consistent-field) method. On the other hand, when the excited state of interest has the same symmetry as the ground-state one has to resort to methods explicitly designed to treat excited states.

Quantum chemical methods used to describe excited states can be roughly categorized in two groups [1]. On the one hand, high-quality wavefunction methods can be used to predict excitation energies and oscillator strengths of low-energy transitions with great accuracy. Among them we find methods based on general multi-configuration SCF (MCSCF) and complete active-space SCF (CASSCF) wavefunctions [2], including the complete active-space second-order perturbation theory (CASPT2) [3]. Equation-of-motion and linear-response coupled-cluster [4, 5], as well as state-universal [6] and state-specific [7] multi-reference coupled cluster, approaches can also be used to describe excited state properties. The symmetry-adapted-cluster configuration interaction (SAC CI) [8] and Green’s function-based methods [9] also deserve notice. All these high-quality wavefunction approaches can be used in small systems, although the meaning of “small” has been adapting to the methodological and algorithmic advances seen in recent decades (see, *e.g.*, Ref. 10). On the other hand, several prominent methods can be used to access excited states at a reduced computational cost, which permits the description of much larger systems. The time-dependent density functional theory (TD-DFT) [11] and configuration-interaction singles (CIS) [12] are perhaps the most widely used methods in this category.

In this work, we describe yet another approach to describe excited states of molecular systems by chains of variational calculations based on symmetry-projected configurations. This approach, first proposed by Schmid and co-workers [13] has already proved successful in the description of excited states in nuclear systems [14]. Recently, we have used the same approach to describe ground and excited states of the two-dimensional periodic Hubbard model [15]. In the excited symmetry-projected HF strategy, each state is described by (a set of) symmetry-projected configurations.

If the states are of the same symmetry, the orthogonality between the states is enforced by a modification of the ansatz. The advantages of this method are several:

- The method can be regarded as having essentially mean-field computational cost.
- Unlike CIS or TD-DFT, the method can describe two-electron excitations with the same ease as one-electron processes.
- One does not need to compromise between the quality of the ground and excited states as is often done in state-averaged MCSCF approaches.
- Being a wavefunction ansatz, the evaluation of response properties and analytic derivative methods are in principle straightforward.

We show the potential of the method in providing a high-quality low-lying spectrum of molecular systems. In particular, we focus on the dissociation profile of the carbon dimer, which is challenging due to the interaction between two low-lying states of the same symmetry. Additionally, we discuss the application of the method to compute the vertical excitation spectrum of formaldehyde. Due to its simplicity, formaldehyde has been studied using a wide variety of theoretical approaches, which facilitates the comparison with other methods. Lastly, we consider a model of the insertion reaction of Be into  $\text{H}_2$ , a challenging system commonly used to assess state-of-the-art quantum chemical methods.

This work is organized as follows. In Sec. II we describe in detail the formalism used in terms of symmetry-projected HF configurations. In Sec. III we briefly describe our implementation of the method. We discuss in Sec. IV the application of the method to the description of the dissociation profile of the carbon dimer, the vertical excitation spectrum of formaldehyde, and the insertion reaction of Be into  $\text{H}_2$ . Sec. V is devoted to concluding remarks.

## II. FORMALISM

We present in this section a detailed account of the formalism employed in this work. We begin in Sec. II A by describing the symmetry-projected HF ansatz for the ground state of a molecular system with well defined quantum numbers. In Sec. II B we set out the excited symmetry-projected HF ansatz for states of the same symmetry as the ground state, an approach introduced by Schmid *et al.* [13]. The variational optimization of the considered wavefunctions is discussed in Sec. II C.

Lastly, in Sec. IID, we describe how one may go about building further correlations in both the ground and excited states [16], even though this is not something we have carried out in this work.

### A. Symmetry-projected Hartree–Fock

In a seminal paper, Löwdin [17] introduced the symmetry-projected HF ansatz for the ground state of a many-body system of fermions. This is expressed as

$$|\Psi\rangle = \hat{P}|\Phi\rangle, \quad (1)$$

where  $\hat{P}$  is a (set of) projection operator(s) that restores the symmetries of a broken symmetry Slater determinant  $|\Phi\rangle$ . This variational ansatz can account for strong correlations due to spin or orbital degeneracies. It is important to stress that, despite the multi-determinantal character in the wavefunction, the ansatz above does not lose the connection to the single-particle picture: the ansatz is fully determined by the set of molecular orbitals occupied in  $|\Phi\rangle$  [18].

In the case of spin projection, Löwdin suggested to use a projection operator of the form

$$\hat{P}^s = \prod_{l \neq s} \frac{\hat{S}^2 - l(l+1)}{s(s+1) - l(l+1)}, \quad (2)$$

where  $s$  is used to label the quantum number to be recovered. The projection operator is written as a product of two-body operators rendering it impractical for routine calculations. Following work from the nuclear physics community, we have discussed in Ref. 19 a more convenient form of the projection operators used for spin and point-group symmetry restoration. These are based on the forms introduced by Bayman [20] (number) and Villars [21] (angular momentum). A similar and earlier spin-projection by rotation formalism introduced by Percus and Rotenberg [22] has gone largely unnoticed. For spin, we use projection-like operators of the form

$$\hat{P}_{mk}^s = \frac{2s+1}{8\pi^2} \int d\Omega D_{mk}^{s*}(\Omega) \hat{R}(\Omega), \quad (3)$$

where  $\Omega = (\alpha, \beta, \gamma)$  is the set of Euler angles parametrizing the rotation in spin space,  $D_{mk}^s(\Omega) \equiv \langle s, m | \hat{R}(\Omega) | s, k \rangle$  is Wigner's  $D$ -matrix, and  $\hat{R}(\Omega)$  is the spin-rotation operator

$$\hat{R}(\Omega) = \exp(-i\alpha\hat{S}_z) \exp(-i\beta\hat{S}_y) \exp(-i\gamma\hat{S}_z). \quad (4)$$

For more details about the form of the projection operators, we refer the reader to Ref. 23. We note that in Ref. [19] we incorrectly suggested that if  $|\Phi\rangle$  is a UHF-type Slater determinant, the projection operator is simplified. While it is true that matrix elements (norm, Hamiltonian) are

simplified (ultimately, a single integration over  $\beta$  is required), the projection operator *does not* change.

In this work, we write the symmetry-projected HF ansatz in the form

$$|\Psi_{j,m}\rangle = \sum_k f_k \hat{P}_{mk}^j |\Phi\rangle, \quad (5)$$

The subscripts  $j, m$  in  $|\Psi\rangle$  label the irreducible representation and the row of the irrep to recover, respectively [24]. The form above is suitable for arbitrary non-Abelian symmetry groups, including spin. The linear variational coefficients  $\{f\}$  are introduced in order to remove unphysical dependencies of the energy with respect to the orientation of the underlying state  $|\Phi\rangle$  [23, 25].

The energy associated with the symmetry-projected HF state of Eq. 5 is given by

$$\begin{aligned} E_j[\Phi] &= \frac{\sum_{kk'} f_k^* f_{k'} \langle \Phi | \hat{P}_{mk}^{j\dagger} \hat{H} \hat{P}_{mk'}^j | \Phi \rangle}{\sum_{kk'} f_k^* f_{k'} \langle \Phi | \hat{P}_{mk}^{j\dagger} \hat{P}_{mk'}^j | \Phi \rangle} \\ &= \frac{\sum_{kk'} f_k^* f_{k'} \langle \Phi | \hat{H} \hat{P}_{kk'}^j | \Phi \rangle}{\sum_{kk'} f_k^* f_{k'} \langle \Phi | \hat{P}_{kk'}^j | \Phi \rangle}, \end{aligned} \quad (6)$$

where we have used the properties of the projection operators [19] and the fact that they commute with the Hamiltonian. We have emphasized the independence of the energy expression on the row of the irrep selected for non-Abelian groups. We discuss in Appendix A the evaluation of norm and Hamiltonian overlaps between symmetry-projected configurations.

In carrying out the optimization of the wavefunction ansatz of Eq. 5, one can consider two possibilities:

- In a projection-after-variation (PAV) approach, the broken-symmetry mean-field state  $|\Phi\rangle$  is optimized variationally. The symmetry-projected energy is then computed in a single-shot evaluation.
- In a variation-after-projection (VAP) approach, the Slater determinant  $|\Phi\rangle$  is optimized in the presence of the projection operators.

The PAV approach is appealing for its simplicity. However, it may lead to unphysical behavior: dissociation profiles evaluated with the PAV approach show derivative discontinuities at the point where the broken-symmetry HF solution collapses back to the symmetry-adapted one [26].

The VAP approach is favored not only because it leads to lower energies, but most importantly because the variation is performed for the actual considered ansatz. As it will be shown below, optimizing the state of Eq. 5 in a VAP manner leads to generalized Brillouin-like conditions that

characterize the stationary nature of the solution. A self-consistent VAP approach was the basis of the extended Hartree–Fock method proposed by Löwdin [17]. More often than not, EHF has been associated with the use of a spin-projection operator on a reference unrestricted determinant (the so-called spin-projected EHF [27]).

Our previous work (Ref. 19) discussed the self-consistent optimization of the symmetry-projected HF approach. In this work, however, we follow a different strategy to carry out the variational optimization, which we describe in more detail in Sec. II C.

## B. The excited symmetry-projected HF approach

Having described the symmetry-projected HF approach for the variational optimization of the ground state of a given symmetry, we now turn our attention to excited states of the same symmetry as the ground state. The excited symmetry-projected HF approach, which relies on a Gram-Schmidt orthogonal construction, was introduced by Schmid *et al.* [13] in the nuclear physics community as the *excited VAMP* (Variation After Mean-field Projection) strategy.

In order for a given ansatz to constitute a faithful representation of an excited state, it must remain orthogonal to the ground state. In variational strategies, this feature may be accomplished in two alternative ways:

- Use the same ansatz as the one employed in the ground state optimization. The orthogonality with respect to the ground state is enforced as a constraint; that is, one minimizes the Lagrangian

$$\mathcal{L}[\Psi] = E[\Psi] - \lambda \langle \Psi | \Psi_0 \rangle, \quad (7)$$

where  $\lambda$  is a Lagrange multiplier and  $|\Psi_0\rangle$  is the ground state.

- Use an ansatz that is explicitly orthogonal to the ground state wavefunction. This is our preferred approach as the minimization problem remains unconstrained.

Let us assume that the symmetry-projected ground state is already available. This we write as

$$\begin{aligned} |\Psi_{j,m}^0\rangle &\equiv |\psi_{j,m}^0\rangle \\ &= \sum_k f_k^0 \hat{P}_{mk}^j |\Phi^0\rangle, \end{aligned} \quad (8)$$

where the 0 superscript is used to denote the ground state character. Our ansatz for the first excited state is given by

$$\begin{aligned} |\Psi_{j,m}^1\rangle &\equiv (1 - \hat{S}^1) |\psi_{j,m}^1\rangle \\ &= (1 - \hat{S}^1) \sum_k f_k^1 \hat{P}_{mk}^j |\Phi^1\rangle, \end{aligned} \quad (9)$$

written in terms of the projector

$$\hat{S}^1 = \frac{|\psi_{j,m}^0\rangle \langle \psi_{j,m}^0|}{\langle \psi_{j,m}^0 | \psi_{j,m}^0 \rangle}, \quad (10)$$

which guarantees the orthogonality of  $|\Psi_{j,m}^1\rangle$  with respect to the ground state. Here, the superscript 1 is used to denote that the first excited state is under consideration. The variational flexibility in the ansatz of Eq. 9 lies in the set of linear variational coefficients  $\{f^1\}$  and the Slater determinant  $|\Phi^1\rangle$ , which is in general not orthogonal to  $|\Phi^0\rangle$ . Nonetheless, it is important to stress that the actual wavefunction is not a single symmetry-projected configuration but a linear combination.

A similar construction can be used for higher excited states. Having the ground state and  $q - 1$  excited states already at our disposal, we prepare an ansatz for the  $q$ -th excited state as

$$\begin{aligned} |\Psi_{j,m}^q\rangle &\equiv (1 - \hat{S}^q) |\psi_{j,m}^q\rangle \\ &= (1 - \hat{S}^q) \sum_k f_k^q \hat{P}_{mk}^j |\Phi^q\rangle, \end{aligned} \quad (11)$$

with the projector  $\hat{S}^q$  given by

$$\hat{S}^q = \sum_{r,s=0}^{q-1} |\psi_{j,m}^r\rangle (A^{-1})_{rs} \langle \psi_{j,m}^s|, \quad (12)$$

$$A_{rs} = \langle \psi_{j,m}^r | \psi_{j,m}^s \rangle. \quad (13)$$

The projector  $\hat{S}^q$  guarantees orthogonality with respect to the ground state and the  $q - 1$  excited states previously considered. We note that, along with the linear coefficients  $\{f^q\}$ , a single Slater determinant  $|\Phi^q\rangle$  determines the full flexibility in the ansatz of Eq. 11. The energy functional associated with the  $q$ -th excited state wavefunction becomes

$$E_j^q[\{f^q\}, |\Phi^q\rangle] = \frac{\sum_{kk'} f_k^{q*} f_{k'}^q \mathcal{H}_{kk'}^q}{\sum_{kk'} f_k^{q*} f_{k'}^q \mathcal{N}_{kk'}^q}, \quad (14)$$

where  $E_j^q$  is the energy of the  $q$ -th excited state. Here, the matrices  $\mathcal{N}^q$  and  $\mathcal{H}^q$  are given by

$$\mathcal{N}_{kk'}^q = \langle \Phi^q | \hat{P}_{km}^j (1 - \hat{S}^q) \hat{P}_{mk'}^j | \Phi^q \rangle, \quad (15a)$$

$$\mathcal{H}_{kk'}^q = \langle \Phi^q | \hat{P}_{km}^j (1 - \hat{S}^q) \hat{H} (1 - \hat{S}^q) \hat{P}_{mk'}^j | \Phi^q \rangle. \quad (15b)$$

We note that even if it may appear otherwise, all matrix elements in the energy functional of Eq. 14 can be evaluated in terms of norm and Hamiltonian overlaps between symmetry-projected configurations (using a single projection operator). For instance,

$$\begin{aligned}\mathcal{N}_{kk'}^q &= \langle \Phi^q | \hat{P}_{km}^j \hat{P}_{mk'}^j | \Phi^q \rangle - \sum_{r,s=0}^{q-1} \sum_{ll'} \langle \Phi^q | \hat{P}_{km}^j \hat{P}_{ml}^j | \Phi^r \rangle (A^{-1})_{rs} \langle \Phi^s | \hat{P}_{l'm}^j \hat{P}_{mk'}^j | \Phi^q \rangle f_l^r f_{l'}^{s*} \\ &= \langle \Phi^q | \hat{P}_{kk'}^j | \Phi^q \rangle - \sum_{r,s=0}^{q-1} \sum_{ll'} \langle \Phi^q | \hat{P}_{kl}^j | \Phi^r \rangle (A^{-1})_{rs} \langle \Phi^s | \hat{P}_{l'k'}^j | \Phi^q \rangle f_l^r f_{l'}^{s*}.\end{aligned}$$

It follows that all states in the irreducible representation  $j$  thereby obtained are degenerate. The expressions used to evaluate matrix elements between symmetry-projected configurations are provided in Appendix A. The variational optimization of the energy functional of Eq. 14 is considered in the following subsection.

Let us assume that, through the scheme described above, the ground state and all  $q$  excited states have already been obtained. These states,  $\{|\Psi_{j,m}^r\rangle | r = 0, \dots, q\}$ , are orthogonal among themselves, but they are not necessarily orthogonal through the Hamiltonian. One can therefore carry out a diagonalization of the Hamiltonian in this basis or, equivalently, in the basis of  $\{|\psi_{j,m}^r\rangle\}$ . The eigenvalue equations can be written as

$$B g = g A \varepsilon, \quad (16)$$

where  $g$  is the matrix of eigenvectors,  $\varepsilon$  is the diagonal matrix of eigenvalues,  $A$  is defined by Eq. 13, and

$$B_{rs} = \langle \psi_{j,m}^r | \hat{H} | \psi_{j,m}^s \rangle. \quad (17)$$

In this way, the states  $\{|\psi_{j,m}^r\rangle\}$  are allowed to interact through the Hamiltonian. The states obtained  $\{|\eta_{j,m}^r\rangle | r = 0, \dots, q\}$  through the diagonalization, expressed as

$$\begin{aligned}|\eta_{j,m}^r\rangle &= \sum_{s=0}^q g_{sr} |\psi_{j,m}^s\rangle \\ &= \sum_{s=0}^q g_{sr} \sum_k f_k^s \hat{P}_{mk}^j | \Phi^s \rangle,\end{aligned} \quad (18)$$

are orthogonal through the Hamiltonian and thus represent a faithful representation of the low-lying spectrum of the considered symmetry. Note also that the final diagonalization of Eq. 16 can account for further correlations in the ground state, that is, beyond those described by the symmetry-projected HF ansatz.

### C. Variational optimization

We proceed to discuss the strategy we use to variationally optimize wavefunctions based on symmetry-projected configurations. Without loss of generality, we work on the optimization of the  $q$ -th excited state wavefunction, whose associated energy functional is given by Eq. 14. The ground state optimization can be carried out in a similar fashion. The optimization has to be performed with respect to the set of linear variational coefficients  $\{f^q\}$  and with respect to the underlying determinant  $|\Phi^q\rangle$ .

The variation of the energy functional (Eq. 14) with respect to  $\{f^{q*}\}$  leads to the generalized eigenvalue problem

$$\sum_{k'} \left( \mathcal{H}_{kk'}^q - E_j^q \mathcal{N}_{kk'}^q \right) f_{k'}^q = 0 \quad \forall \quad k, \quad (19)$$

which has to be solved subject to the normalization constraint

$$f^{q\dagger} \mathcal{N}^q f^q = \mathbf{1}_{d'}, \quad (20)$$

where  $d' \leq d$  and  $d$  is the dimension of the irreducible representation recovered by the projection. The Hamiltonian  $\mathcal{H}^q$  and overlap  $\mathcal{N}^q$  matrices are given by Eqs. 15b and 15a, respectively. In addition,  $E_j^q$  is the lowest-energy solution to the eigenvalue problem (it constitutes the energy of the  $q$ -th excited state); all other solutions are discarded at this point.

The variation of the energy functional with respect to the underlying determinant,  $|\Phi^q\rangle$ , is more convoluted. We use a parametrization based on the Thouless theorem, which states that the  $N$ -electron Slater determinant  $|\Phi^q\rangle$  can be written in terms of another (reference)  $N$ -electron Slater determinant  $|\Phi\rangle$  as

$$|\Phi^q\rangle = \eta \exp(\hat{Z}^q) |\Phi\rangle, \quad (21)$$

$$\hat{Z}^q = \sum_{ph} Z_{ph}^q b_p^\dagger b_h, \quad (22)$$

as long as  $|\Phi^q\rangle$  is not orthogonal to  $|\Phi\rangle$ . Here,  $\eta = \langle \Phi^q | \Phi \rangle$  is a normalization factor, and the sum in Eq. 22 is over particle and hole operators defined by the orbitals characterizing  $|\Phi\rangle$ . The coefficients  $Z_{ph}^q$  are unique.

The Thouless theorem permits an efficient parametrization of the Slater determinant  $|\Phi^q\rangle$ . That is, we use Eq. 21 and treat the coefficients  $Z_{ph}^q$  as variational parameters. We note that this Thouless parametrization has not been frequently used in chemistry. Mang [28], among others, suggested its use in the nuclear physics community in the context of a Hartree–Fock–Bogoliubov reference

vacuum. Recently, Noga and Šimunek [29] used a Thouless matrix, in a unitary coupled-cluster singles framework, to carry out the optimization of independent particle model wavefunctions. Their approach is similar in spirit to ours, though the actual algorithm has important differences. A Thouless-based optimization is also closely related to the quadratically-convergent algorithm suggested by Backsay [30]. We point the interested reader to Refs. 31 and 32 for a more detailed description of the approach we use.

Using Eq. 21, we can write the energy functional of Eq. 14 as one depending on the coefficients  $Z_{ph}^q$ ,

$$E_j^q[\{f^q\}, Z^q] = \frac{\sum_{kk'} f_k^{*q} f_{k'}^q \langle \Phi | \exp(\hat{Z}^{q\dagger}) \hat{P}_{km}^j (1 - \hat{S}^q) \hat{H} (1 - \hat{S}^q) \hat{P}_{mk'}^j \exp(\hat{Z}^q) | \Phi \rangle}{\sum_{kk'} f_k^{*q} f_{k'}^q \langle \Phi | \exp(\hat{Z}^{q\dagger}) \hat{P}_{km}^j (1 - \hat{S}^q) \hat{P}_{mk'}^j \exp(\hat{Z}^q) | \Phi \rangle}, \quad (23)$$

where  $|\Phi\rangle$  is an arbitrary reference state used for the minimization.

A stationary point of the energy functional of Eq. 23 is reached when the energy gradient, given by

$$\begin{aligned} G_{ph}^q &\equiv \frac{\partial}{\partial Z_{ph}^{q*}} E_j^q[\{f^q\}, Z^q] \\ &= \frac{\sum_{kk'} f_k^{*q} f_{k'}^q \langle \Phi^q | b_h^\dagger b_p \hat{P}_{km}^j (1 - \hat{S}^q) (\hat{H} - E_j^q) (1 - \hat{S}^q) \hat{P}_{mk'}^j | \Phi^q \rangle}{\sum_{kk'} f_k^{*q} f_{k'}^q \langle \Phi^q | \hat{P}_{km}^j (1 - \hat{S}^q) \hat{P}_{mk'}^j | \Phi^q \rangle}, \end{aligned} \quad (24)$$

vanishes for all elements of  $G^q$ . Here, the HF operators  $b_h^\dagger$  and  $b_p$  are associated with the determinant  $|\Phi\rangle$  (and not  $|\Phi^q\rangle$ ). This is sometimes referred to as the global gradient. The local gradient  $\mathcal{G}^q$  at  $|\Phi\rangle = |\Phi^q\rangle$ , given by

$$\begin{aligned} \mathcal{G}_{ph}^q &\equiv \left. \frac{\partial}{\partial Z_{ph}^{q*}} E_j^q[\{f^q\}, Z^q] \right|_{Z_{ph}^q=0} \\ &= \frac{\sum_{kk'} f_k^{*q} f_{k'}^q \langle \Phi^q | b_h^{q\dagger} b_p^q \hat{P}_{km}^j (1 - \hat{S}^q) (\hat{H} - E_j^q) (1 - \hat{S}^q) \hat{P}_{mk'}^j | \Phi^q \rangle}{\sum_{kk'} f_k^{*q} f_{k'}^q \langle \Phi^q | \hat{P}_{km}^j (1 - \hat{S}^q) \hat{P}_{mk'}^j | \Phi^q \rangle}, \end{aligned} \quad (25)$$

in which HF operators associated with  $|\Phi^q\rangle$  are used, can be related to the global gradient by [33]

$$G^q = \tilde{L}^{\text{T}-1} \mathcal{G}^q L^{*-1}. \quad (26)$$

Here,  $\tilde{L}$  and  $L$  are  $(M - N) \times (M - N)$  and  $N \times N$  matrices, respectively, obtained from standard Cholesky decompositions (see Ref. 33). We note that the local gradient also vanishes at a stationary point of the energy functional.

Once the optimal  $|\Phi^q\rangle$  has been found, it is convenient to have a unique representation of the molecular orbitals characterizing the Slater determinant (recall that the functional is invariant to unitary transformations among the occupied orbitals). This can be accomplished by diagonalizing the  $H^{11}$  sector of the Hamiltonian, whose hole-hole and particle-particle blocks are given by

$$H_{hh'}^{11} = \langle \Phi^q | b_h^\dagger H b_{h'} | \Phi^q \rangle - \delta_{hh'} \langle \Phi^q | \hat{H} | \Phi^q \rangle, \quad (27a)$$

$$H_{pp'}^{11} = \langle \Phi^q | b_p H b_{p'}^\dagger | \Phi^q \rangle - \delta_{pp'} \langle \Phi^q | \hat{H} | \Phi^q \rangle. \quad (27b)$$

Note that this is simply a way of finding semi-canonical orbitals, using traditional quantum chemical jargon.

We close this section by listing some of the advantageous features that a variational optimization based on a Thouless parametrization provides:

- The minimization problem is unconstrained, with as many parameters as linearly independent variables. Powerful algorithms (conjugate gradient, quasi-Newton methods) for unconstrained minimization can be used [34].
- Because of the gradient-based approach used, one is guaranteed that the optimization will either converge to a stationary point within a specified tolerance or the algorithm used will fail.
- The application of the method to symmetry-projected approaches or arbitrary wavefunctions expressed in terms of Slater determinants is straightforward.
- The method does not require one to *a priori* decide how to occupy the orbitals, which a diagonalization approach requires. For HF, an *aufbau* occupation leads to the lowest energy solution, but the same need not be true for more general functionals.

#### D. Correlations in the ground and excited states

In the previous sections, we have considered an ansatz for the ground and excited states of a given symmetry. Each state is described by essentially a single symmetry-projected HF configuration. If this description proves insufficient, one can consider a more general ansatz written as a linear combination of symmetry-projected configurations as a trial wavefunction for each state. This approach has been used to describe ground-state correlations of molecular systems in Ref. 35 and in the Hubbard model in Ref. 16. We briefly describe the idea in this section, even though we do not include results from such multi-component approach in our calculations.

In a multi-component approach, the ground state is expanded as a linear combination of symmetry-projected configurations

$$\begin{aligned} |\Psi_{j,m}^0\rangle &\equiv |\psi_{j,m}^0\rangle \\ &= \sum_k \hat{P}_{mk}^j \sum_{z=1}^{n_0} f_{z;k}^0 |\Phi_z^0\rangle. \end{aligned} \quad (28)$$

Here, once again the superscript 0 denotes the ground state character of the considered ansatz. The trial wavefunction is expanded as a linear combination of  $n_0$  symmetry-projected configurations, obtained from the corresponding set of (non-orthogonal) Slater determinants  $\{|\Phi_z^0\rangle \mid z = 1, \dots, n_0\}$ .

The ansatz for the  $q$ -th excited state is similar to that from the single-configuration approach. It is given by

$$\begin{aligned} |\Psi_{j,m}^q\rangle &\equiv (1 - \hat{S}^q) |\psi_{j,m}^q\rangle \\ &= (1 - \hat{S}^q) \sum_k \hat{P}_{mk}^j \sum_{z=1}^{n_q} f_{z;k}^q |\Phi_z^q\rangle, \end{aligned} \quad (29)$$

with the projector  $\hat{S}^q$  given by an expression analogous to Eq. 12. (Note, nonetheless, that each state  $|\psi_{j,m}^r\rangle$  is given by a linear combination of  $n_r$  symmetry-projected configurations.)

One may now wonder how the variational optimization is performed in this multi-component approach. The two extreme strategies are:

- All the determinants  $\{|\Phi_z^q\rangle \mid z = 1, \dots, n_q\}$  describing the  $q$ -th excited state are optimized at once. This is known in the literature as the resonating Hartree–Fock approach (Res HF), first introduced by Fukutome [36].
- A step-wise construction is used in which only the last added determinant is optimized while the previously obtained remain frozen. This is known, in the nuclear physics community, as the few-determinant (FED) approach introduced by Schmid *et al.* [37]. In combination with the Gram-Schmidt orthogonal construction used for the excited states, it is referred to as the *excited FED VAMP* strategy [37]. We note that a similar approach, even if Slater determinants were used in place of the symmetry-projected configurations, was employed by Koch and Dalgaard [38] in ground state optimizations.

We refer the reader to our recent work on the one-dimensional Hubbard Hamiltonian [16] where the merits of this approach have been discussed.

### III. COMPUTATIONAL DETAILS

We have developed a computer program that can optimize symmetry-projected HF states (as well as excited states) using a Thouless parametrization, as described in Sec. II C. This is different from our original work (see Ref. 19), which used a diagonalization based approach. A limited-memory Broyden–Fletcher–Goldfarb–Shanno (BFGS) [39, 40] quasi-Newton method is used as the unconstrained minimization algorithm. The program interfaces with the `GAUSSIAN` suite [41] to retrieve one- and two-electron integrals. Our program is parallelized (MPI-based) over the grid to perform the symmetry restoration (spatial and/or spin). We note that if a single symmetry-projected configuration is used to describe each state (as done in this work), the excited method scales linearly with the order of the state described. That is, the optimization of the first excited state is twice as expensive as that of the ground state. Unfortunately, we have not yet implemented the capability of evaluating oscillator strengths of the excited states, but it is straightforward to do so once the appropriate integrals are available. We prepare an initial guess for the broken symmetry determinants by taking the converged HF solution and mixing a few orbitals closest to the Fermi energy using a randomly prepared unitary matrix. A similar strategy has been used in our recent study of the one-dimensional Hubbard model [16].

### IV. RESULTS AND DISCUSSION

We discuss the application of the excited symmetry-projected HF method to three different systems: the dissociation profile of the carbon dimer, the vertical excitation spectrum of formaldehyde, and a model for the insertion reaction of Be in  $\text{H}_2$ . We consider simple systems in small basis in order to compare with previously reported results. Lastly, we emphasize that, in order to showcase the excited symmetry-projected HF strategy, it has to be applied to systems for which a few excited states of the same symmetry are of interest.

#### A. Dissociation profile of the carbon dimer

We consider the dissociation profile of the carbon dimer in the 6-31G(d) basis, for which the full CI (FCI) dissociation profile was reported by Abrams and Sherrill in Ref. [42]. The correct description of the dissociation profile of the carbon dimer is quite challenging from a theoretical point of view: not only is a double-bond being broken, but there is a low-lying excited state of the same-symmetry ( $^1\Sigma_g^+$ ) as the ground state nearby in energy. In fact, an avoided crossing occurs at

$\approx 1.7 \text{ \AA}$ , where the character of the two states is interchanged. In addition, there is also a low-lying  $^1\Delta_g$  state that becomes the ground state at large interatomic separation. A further complication arises because, as described by Abrams and Sherrill, within the  $D_{2h}$  subgroup available in most quantum chemical packages, the  $^1\Sigma_g^+$  and the  $^1\Delta_g$  states have the same  $^1A_g$  symmetry [42].

An assessment of the ability of several sophisticated quantum chemical methods to describe the dissociation profile was presented in Refs. [42] and [43]. Most coupled-cluster approaches fail to provide even a qualitatively correct description of the dissociation profile of the ground state, with its characteristic non-Morse-like behavior due to the avoided crossing. Only multi-reference approaches such as CASPT2 or multi-reference CI [43] can accurately describe the dissociation profile of all three states considered.

The dissociation profile of four low-lying singlet states of  $C_2$  as predicted with the excited  $D_{4h}$ S-UHF method is shown in Fig. 1. Here, the  $D_{4h}$ S-UHF notation implies that spin projection (S) and spatial symmetry-restoration (in the  $D_{4h}$  point group) have been broken and restored from an underlying determinant of unrestricted HF (UHF) character. The use of the  $D_{4h}$  subgroup allows us to distinguish between the  $^1\Sigma_g^+$  and the  $^1\Delta_g$  irreducible representations of the  $D_{\infty h}$  group: the  $^1\Delta_g$  state transforms as the  $^1B_{1g}$  irreducible representation in the  $D_{4h}$  subgroup. For the two  $^1A_{1g}$  states we show the profiles obtained before (top panel) and after (bottom panel) they are allowed to interact through the Hamiltonian in the final diagonalization of Eq. 16.

Several features of the exact dissociation profile are correctly described with our  $D_{4h}$ S-UHF approximation. In particular, we observe that the  $B_{1g}$  state is correctly predicted to be the lowest energy state for  $r_{C-C} > 1.6 \text{ \AA}$ . The avoided crossing observed in the FCI profile appears after the two  $^1A_{1g}$  symmetry-projected configurations are allowed to interact. In this way, the dissociation profile predicted for the lowest-lying  $^1A_{1g}$  state correctly displays the characteristic non-Morse-like behavior. One should note, however, that the carbon-carbon distance of closest approach between the two  $^1A_{1g}$  states is slightly larger than in the FCI solution. We finally point out that the curves obtained for the three states for which the FCI solution is available are fairly parallel to the latter. This validates our description of the ground and excited states of  $C_2$  in terms of symmetry-projected configurations. We emphasize that essentially a single symmetry-projected configuration was used for each state: two symmetry-projected configurations were used to describe two states of  $^1A_{1g}$  symmetry.

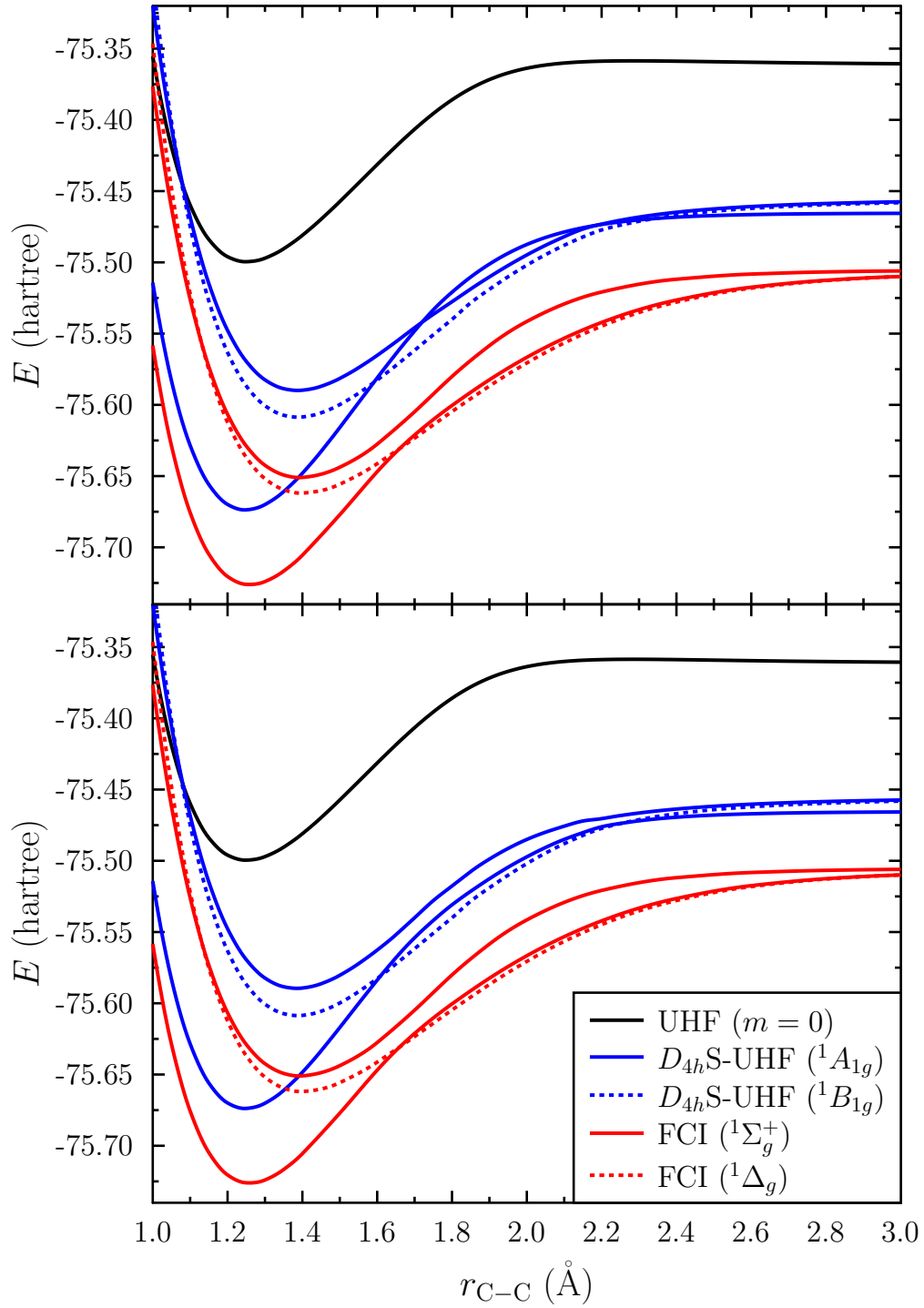


FIG. 1. Dissociation profiles for low-lying singlet states of the  $C_2$  molecule computed with the  $D_{4h}S$ -UHF / 6-31G(d) method. A comparison with FCI curves from Ref. [42] is shown. The  $D_{4h}S$ -UHF profiles for the two  $^1A_{1g}$  states as obtained before (top panel) and after (bottom panel) the final diagonalization (Eq. 16) are displayed. The avoided crossing is correctly described after the two  $^1A_{1g}$  states are allowed to interact through the Hamiltonian.

## B. Vertical excitation spectrum of formaldehyde

Formaldehyde is the simplest of the carbonyl compounds and as such it is ubiquitous in nature. The presence of a  $\pi$ -electron system and the lone pairs of oxygen permit  $n \rightarrow \pi^*$  and  $\pi \rightarrow \pi^*$  valence transitions, making formaldehyde photochemically active. Because of its small size and availability, formaldehyde has been widely studied both experimentally and theoretically.

Some vertical excitation transitions of formaldehyde have been experimentally determined (see Refs [44] and [45]). The vertical excitation spectrum of formaldehyde has been studied theoretically by several authors, both to help in the assignment of the spectrum, as well as to test different theoretical approaches. We refer the reader to the work by Hadad *et al.* [46], Pitarch-Ruiz *et al.* [47], and references therein. Recently, Schreiber *et al.* [48] have provided best theoretical estimates for some low-energy valence and Rydberg transitions of formaldehyde.

Our focus here is to test whether our approach can provide reasonable excitation energies. In particular, we focus on the vertical excitation spectrum as we currently lack the ability to optimize the geometries of ground and excited states. We use the ground state  $C_{2v}$  geometry from Ref. [46] (optimized with MP2/6-31G(d)). The basis set 6-311(2+,2+)G(d,p) we use was also obtained from the same work. The second set of diffuse functions was found necessary in order to correctly describe the Rydberg transitions at the CIS level.

In Fig. 2 we show how six different singlet  $A_1$  states are obtained by the chain of variational calculations defined in the excited symmetry-projected ( $C_{2v}$ S-UHF) approach. Here, the notation  $C_{2v}$ S-UHF implies that spin and spatial symmetry (in the  $C_{2v}$  framework) is restored from a broken symmetry UHF-type determinant. Observe that the states are not necessarily obtained in a strict increasing-energy order. In our  $C_{2v}$ S-UHF calculations for triplet states, we have used an  $m_s = 1$  UHF-type determinant; the use of  $m_s = 0$  determinants would lead to different results [49]. The right-most column shows the resulting set of states after the final diagonalization of Eq. 16. In this particular case, the ground state gains almost no additional correlations as it is well separated from other states energetically. On the other hand, several of the states interact strongly as evidenced by the large differences observed from column 6 to the column labeled as “final”.

We show, in Fig. 3 the full low-lying singlet and triplet vertical spectrum of formaldehyde predicted with the  $C_{2v}$ S-UHF approach. A comparison with experimental results from Refs. 44 and 45 and a few other results compiled in Ref. 46 is also provided. As we have used a limited basis set and our treatment of electron correlation is only approximate, we cannot expect perfect agreement with experimental numbers. The agreement between our  $C_{2v}$ S-UHF and the experi-

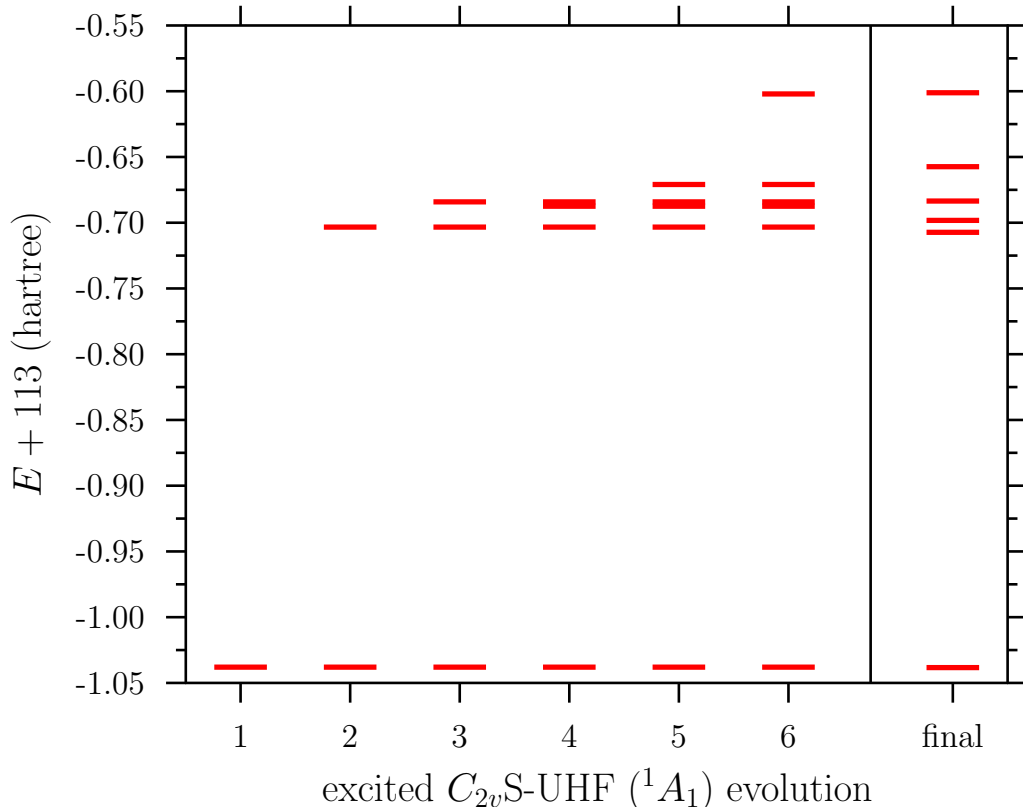


FIG. 2. Evolution of the  $^1A_1$  spectrum of formaldehyde as computed with the excited  $C_{2v}$ S-UHF method with increasing number of symmetry-projected configurations. The last column shows the spectrum obtained after the final diagonalization of Eq. 16 is carried out.

mental excitation energies (for both singlet and triplet states) is remarkable, as each of the states obtained is described by essentially a single symmetry-projected configuration. There is no *a priori* reason to expect that all states should be well approximated by a single symmetry-projected configuration, or that the quality obtained for the different irreducible representations should be comparable. Nevertheless, the agreement with the experimental excitation energies is quite good, with maximum deviations of  $\approx 1$  eV for both singlet and triplet states.

We show in Table I a comparison of the predicted low-lying vertical excitation of formaldehyde with  $C_{2v}$ S-UHF and other results available from the literature. In particular, we compare with the CIS and CIS-MP2 results of Ref. [46], where the latter includes an electron correlation correction to the CIS energies via perturbation theory through second order, and with the (SC)<sup>2</sup> multi-reference (MR) CI with singles and doubles (SD) of Ref. [47], which constitute best available theoretical estimates. The (SC)<sup>2</sup> scheme is a self-consistent dressing procedure that, among other effects, corrects the size-extensivity of MR-CI [50]. The CIS and CIS-MP2 calculations use the same

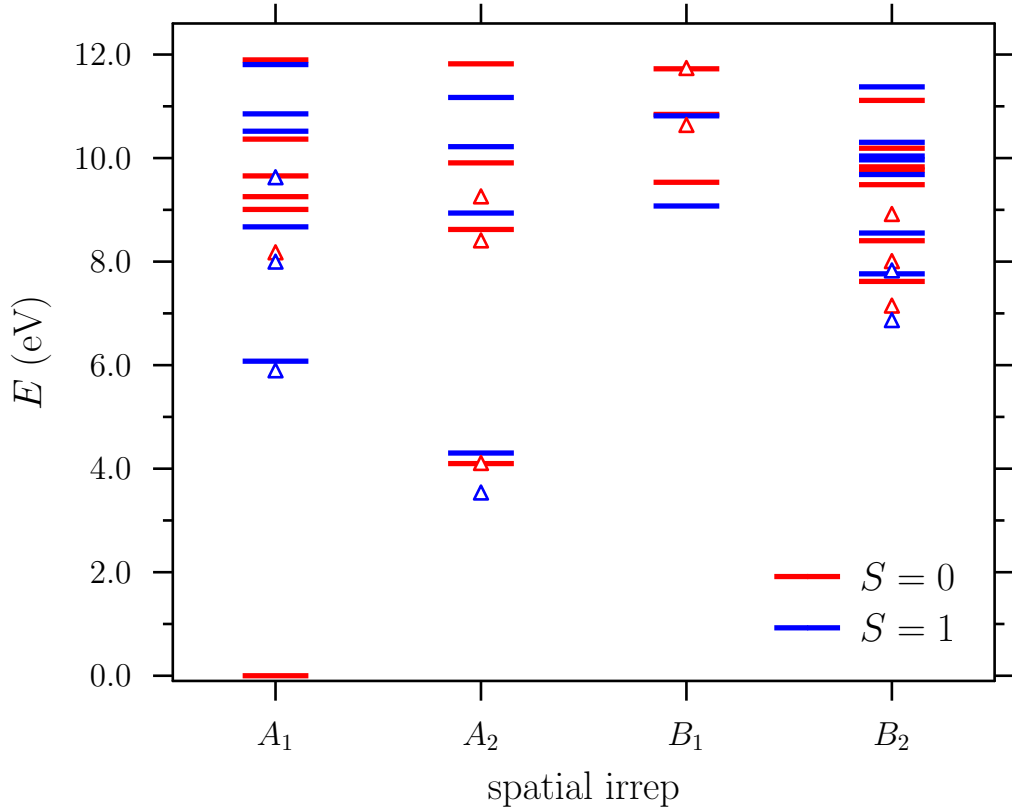


FIG. 3. Low-lying singlet and triplet states of the formaldehyde molecule predicted with the  $C_{2v}$ S-UHF method. The 6-311(2+,2+)G(d,p) basis was used in the calculations. Experimental excitation energies from Refs. 44–46 are shown as red and blue triangles for singlet and triplet states, respectively.

basis set and geometry that we have used. The MR-CISD calculations use a large atomic natural-orbital-type  $[6s5p3d2f/4s3p2d]$  basis for C,O/H augmented with a  $3s3p3d$  adapted Rydberg series. The latter diffuse functions were placed in the charge center of the  $^2B_2$  state of the formaldehyde cation. The ground-state geometry used in MR-CISD calculations was described in Ref. 47; it deviates  $\approx 0.01\text{\AA}$  in bond-lengths and  $\approx 1^\circ$  in the H-C-H angle with respect to the MP2/6-31G(d) optimized geometry. The states in Table I are ordered according to:

- The CIS and CIS-MP2 states are listed in increasing order according to the CIS-MP2 excitation energies.
- Experimental vertical excitations are listed according to the assignment provided in Ref. 46 with respect to CIS results.
- MR-CISD results are listed in increasing order, trying to match the assignments provided in Ref. 47 with those in Ref. 46.

- The  $C_{2v}$ S-UHF excitation energies are listed in increasing order as we have not tried to make a formal assignment of the excitation energies. Such an assignment would only provide a guide for interpretation as states of the same symmetry always possess mixed character.

TABLE I. Vertical excitation energies (in eV) of formaldehyde as predicted by the excited  $C_{2v}$ S-UHF, CIS, CIS-MP2, and (SC)<sup>2</sup>-MR-CISD methods compared to the available experimental data. The states are listed according to their spin and spatial-symmetry labels. (See text for a description of the ordering used in listing the states.)

label	singlets					triplets				
	EPHF <sup>a</sup>	CIS <sup>b</sup>	CIS-MP2 <sup>b</sup>	MRCI <sup>c</sup>	expt <sup>d</sup>	EPHF <sup>a</sup>	CIS <sup>e</sup>	CIS-MP2 <sup>b</sup>	MRCI <sup>c</sup>	expt <sup>d</sup>
$A_1$	9.01	9.66	8.47	8.27	8.14	6.08	4.65	6.72	6.05	5.86
	9.25	10.88	8.75	9.31		8.67	9.31	7.78	8.15	
	9.66	9.45	9.19	9.68		10.52	10.56	9.12	9.35	
	10.37	11.24	9.20			10.85	10.88		9.64	
	11.90	12.09	9.99			11.81	11.89			
$A_2$	4.10	4.48	4.58	4.04	4.07	4.30	3.67	4.15	3.59	3.50
	8.62	9.78	7.83	8.36		8.94	9.72	8.16	8.41	
	9.91	10.92	10.08	9.34		10.22	10.20	10.52	9.37	
	11.82	12.06	10.13			11.17	11.15			
		11.37	10.49							
$B_1$		11.93	11.63							
	9.53	9.66	9.97	9.33	10.60	9.07	8.37	9.18	8.52	9.33
	10.84	11.05	10.84			10.82	10.86			
$B_2$	11.72	11.84	11.56			13.75	11.56			
	7.62	8.63	6.85	7.12	7.11	7.76	8.28	6.97	6.98	6.83
	8.40	9.36	7.66	7.95		8.55	9.04	7.75	7.81	
	9.49	10.61	8.46	8.96		9.68	10.33	8.67	8.83	
	9.77	10.86	8.94	9.18		9.97	10.69		9.16	
	9.83	10.98	8.96	9.27		10.04	10.80			
	10.19	11.17	9.19			10.30	11.07			
	11.11					11.38				

<sup>a</sup>  $C_{2v}$ S-UHF; this work.

<sup>b</sup> From Ref. 46.

<sup>c</sup> (SC)<sup>2</sup>-MR-CISD results from Ref. 47.

<sup>d</sup> Experimental excitation energies from Refs. 44–46.

<sup>e</sup> CIS; this work.

The results shown in Table I show a surprisingly good qualitative agreement between our  $C_{2v}$ S-UHF calculations and the MR-CISD and experimental vertical excitation energies. In particular, the  $C_{2v}$ S-UHF results significantly improve over CIS for most of the excitations listed in the table.

Larger deviations are observed for states with significant Rydberg character, suggesting that the basis set used is still not sufficient to converge such excitation energies. The observed agreement between  $C_{2v}$ -UHF excitation energies with best theoretical estimates is encouraging as it showcases the ability of the simple, mean-field excited symmetry-projected HF approach to describe excited states of molecular systems.

### C. $C_{2v}$ insertion pathway for BeH<sub>2</sub>

The model  $C_{2v}$  insertion pathway of Be into H<sub>2</sub> is a known challenging system. It was originally proposed by Purvis *et al.* [51] as testing ground for single-reference coupled-cluster methods. It has recently been used as a benchmarking case for novel multi-reference based methods (see Ref. 52 and references therein).

We follow Ref. 52 in the construction of the model pathway: with the beryllium atom placed at the origin, the  $y$  coordinates (in bohr) of the hydrogen atoms are related to their  $x$  coordinates (in bohr) by the equation

$$y(x) = \pm(2.54 - 0.46x) \quad x \in [0, 4].$$

At  $x = 0$ , the geometry described corresponds approximately to the BeH<sub>2</sub> equilibrium geometry, while at  $x = 4$ , the geometry corresponds to a hydrogen molecule at equilibrium interacting with a Be atom placed 4 bohr away. A linear interpolation is used for intermediate geometries; the model insertion pathway has  $C_{2v}$  symmetry. In our calculations, we use the same small basis set as that used in Ref. 52, corresponding to the contraction scheme Be(10s3p/3s2p) and H(4s/2s).

The BeH<sub>2</sub> model insertion pathway is challenging as the dominant configurations in the FCI expansion change character. At the equilibrium BeH<sub>2</sub> geometry, the dominant configuration is

$$(1\sigma_g)^2 (2\sigma_g)^2 (1\sigma_u)^2 \quad \equiv \quad (1a_1)^2 (2a_1)^2 (1b_2)^2,$$

where the l.h.s. configuration uses the  $D_{\infty h}$  symmetry of the linear molecule and the r.h.s. is its representation in the  $C_{2v}$  subgroup. On the other hand, at dissociation, the dominant configuration becomes

$$(1a_1)^2 (2a_1)^2 (3a_1)^2.$$

Note that the latter corresponds to a double excitation with respect to the reference determinant near the BeH<sub>2</sub> equilibrium. Excited state methods based on a particle-hole construction out of

a symmetry-adapted reference would therefore fail to provide even a qualitatively correct profile for the first excited state. Single-reference coupled-cluster can correctly describe the ground-state dissociation pathway only when different references are used in different intervals of  $x$  [51, 52]; the resulting curve is, nevertheless, discontinuous. We note that different flavors of multi-reference coupled-cluster can correctly describe the model insertion pathway [52].

We show in Fig. 4 the insertion pathways predicted by UHF,  $C_{2v}$ S-UHF, and  $C_{2v}$ KS-UHF, as a function of the  $x$  coordinate of the hydrogen atoms. In  $C_{2v}$ S-UHF, the full-spin symmetry and the spatial symmetry ( $C_{2v}$ ) are broken and restored self-consistently; in  $C_{2v}$ KS-UHF, we additionally break and restore complex conjugation (denoted by K). We also present the ground state FCI curve (obtained from Ref. 52) for comparison purposes.

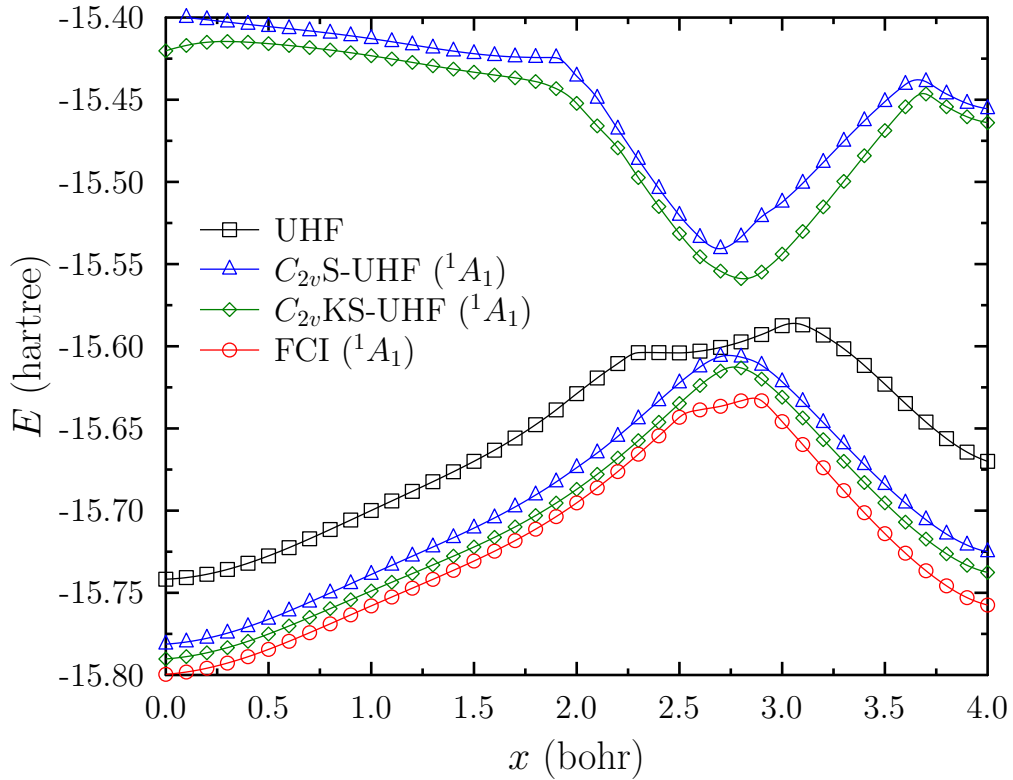


FIG. 4. Model  $C_{2v}$  insertion pathway of Be into  $H_2$  as a function of the  $x$ -coordinate of the hydrogen atoms (Be is placed at the origin). The FCI results were obtained from Ref. 52. Note that  $C_{2v}$ S-UHF and  $C_{2v}$ KS-UHF predict smooth curves for the two low-lying  $^1A_1$  states.

As Fig. 4 shows, both excited symmetry-projected HF approaches provide smooth curves for both the ground state and the first excited state. The obtained curves display the interaction between the lowest  $^1A_1$  states in the model reaction pathway. Moreover, the profiles are qualitatively

similar to the CASSCF and FCI curves reported in Ref. 51 for both states. The  $C_{2v}$ KS-UHF curve lies very close to the FCI curve in the interval  $x < 2.5$ . Near  $x \approx 2.7$ , where the multi-reference character is expected to be highest as the different configurations interact strongly, both  $C_{2v}$ S-UHF and  $C_{2v}$ KS-UHF deviate from the ground state FCI curve. We stress, nevertheless, that our results can be improved by: a) using more symmetry-projected configurations for each state, and b) including more states in the excited symmetry-projected HF approach.

## V. CONCLUSIONS

The spectrum of a molecular system constitutes the fingerprint of its quantum mechanical character. Characterization of the low-lying excited states of a system is of paramount importance in order to understand photochemical and photophysical processes occurring in nature. Accessing an excited state of the same symmetry as the ground state has always been challenging for variational strategies. This is because, if the optimization is carried out using the same formalism as that used for the ground state, a variational collapse is almost inevitable. In the formalism discussed in this work we avoided this collapse by using an ansatz that is explicitly orthogonal to states of the same symmetry previously obtained. We note that the Gram-Schmidt orthogonal construction used in this work in terms of symmetry-projected configurations could be used with other types of wavefunction.

In a nutshell, our formalism uses chain of variational calculations to characterize the low-lying excited states of a system with a given set of quantum numbers in terms of symmetry-projected configurations. The use of the latter implies that the wavefunctions thus obtained have well defined symmetries.

We have applied the excited symmetry-projected HF formalism to describe the dissociation profile of the  $C_2$  molecule, to characterize the low-lying spectrum of formaldehyde, and to explore a model insertion pathway for  $BeH_2$ . Several features of the potential energy curve of the carbon dimer were correctly reproduced; in particular, the non-Morse shape of the lowest lying  $A_1$  state is obtained after the two symmetry-projected configurations are allowed to interact. This constitutes the avoided crossing also observed with other multi-configurational methods such as MRCI or CASPT2. The low-lying singlet and triplet spectrum of formaldehyde was characterized and compared with available experimental adiabatic excitation energies. We have observed a good agreement between our computed spectrum and the experimental one (all excitation energies are correct within a  $\approx 1$  eV window). This is remarkable given that each state was essentially described

by a single-symmetry projected configuration, that is, we solved for as many states as the amount of symmetry-projected configurations we used.

The methodology here considered can be applied to larger systems as it has mean-field cost. We believe that this method can become a useful tool for the computational chemist. It may be used to fill the void between the high-accuracy methods and the large-scale methods, where the latter typically assume a particle-hole character for the low-lying excited states.

## ACKNOWLEDGMENTS

This work was supported by the Department of Energy, Office of Basic Energy Sciences, Grant No. DE-FG02-09ER16053. G.E.S. is a Welch Foundation Chair (C-0036). C.A.J.H. acknowledges support from the Lodieska Stockbridge Vaughn Fellowship.

## Appendix A: Matrix elements between symmetry-projected configurations

In this appendix, we provide explicit expressions for matrix elements required in the evaluation of the energy and the energy gradient of wavefunctions based on symmetry-projected configurations. As shown below, these can be in turn written in terms of matrix elements between (non-orthogonal) rotated Slater determinants. Löwdin [53] first described the evaluation of arbitrary operator matrix elements between non-orthogonal  $N$ -electron Slater determinants. An extended Wick’s theorem can be used to evaluate such matrix elements as shown by, *e.g.*, Blaizot and Ripka [54].

We begin by describing the notation used. We work with a set of  $M$  elementary fermion creation  $\{c^\dagger\}$  and annihilation  $\{c\}$  operators satisfying the standard anti-commutation rules

$$\left[ c_j, c_k \right]_+ = 0, \quad (\text{A1a})$$

$$\left[ c_j^\dagger, c_k^\dagger \right]_+ = 0, \quad (\text{A1b})$$

$$\left[ c_j, c_k^\dagger \right]_+ = \langle j|k \rangle = \delta_{jk}. \quad (\text{A1c})$$

Note that an orthonormal basis is used. The transformation from the non-orthogonal atomic orbital basis to an orthonormal one is straightforward.

The non-relativistic, Born-Oppenheimer molecular electronic Hamiltonian  $\hat{H}$  is expressed in second quantization as

$$\hat{H} = \sum_{ik} \langle i|\hat{h}|k \rangle c_i^\dagger c_k + \frac{1}{4} \sum_{ijkl} \langle ij|\hat{v}|kl \rangle c_i^\dagger c_j^\dagger c_l c_k, \quad (\text{A2})$$

where  $\langle i|\hat{h}|k\rangle$  are one-electron (core Hamiltonian) integrals and  $\langle ij|\hat{v}|kl\rangle$  are anti-symmetrized two-electron (electron repulsion) integrals in Dirac notation.

An arbitrary  $N$ -electron Slater determinant  $|\Phi\rangle$  is constructed as a vacuum to a set of  $N$  occupied (hole) HF creation operators  $\{b_h^\dagger | h = 1, \dots, N\}$  and  $M - N$  virtual (particle) HF annihilation operators  $\{b_p | p = N + 1, \dots, M\}$ . It may be represented as

$$|\Phi\rangle = \prod_{h=1}^N b_h^\dagger |-\rangle, \quad (\text{A3})$$

where  $|-\rangle$  is the bare fermion vacuum (annihilated by  $\{c\}$ ). The HF operators are given as linear combinations of the elementary fermion ones, that is,

$$b_k^\dagger = \sum_j D_{jk}^* c_j^\dagger, \quad (\text{A4})$$

where  $D$  is the matrix of molecular orbital coefficients. (Note that our choice for the matrix of orbital coefficients is the complex conjugate of the standard one.) As usual, the first  $N$  columns in  $D$  are used for the occupied molecular orbitals, while the remaining columns describe the virtual orbitals. The above transformation is canonical (it preserves fermion anti-commutation rules) if the matrix  $D$  is unitary:  $D D^\dagger = D^\dagger D = \mathbf{1}$ .

In order to provide explicit expressions for the matrix elements, we introduce a generic form of the projection operator  $\hat{P}_{mk}^j$  (for general non-Abelian groups) given by

$$\hat{P}_{mk}^j = \frac{1}{V} \int_V d\vartheta w_{mk}^j(\vartheta) \hat{R}(\vartheta). \quad (\text{A5})$$

A state transforming as the  $m$ -th row of the  $j$ -th irreducible representation is recovered upon the action of the above projection operator on an arbitrary state. Here,  $\vartheta$  labels the elements of the symmetry group; for discrete groups, the integration should be understood as a summation. In addition,  $V$  is the volume of integration,  $w_{mk}^j(\vartheta)$  is an integration weight (character) associated with the symmetries of the state to be recovered, and  $\hat{R}(\vartheta)$  is a rotation operator.

For all the cases considered in this work,  $\hat{R}(\vartheta)$  is a single-particle rotation operator that transforms the HF operators according to

$$\begin{aligned} b_k^\dagger(\vartheta) &\equiv \hat{R}(\vartheta) b_k^\dagger \hat{R}^{-1}(\vartheta) \\ &= \sum_j D_{jk}^* \hat{R}(\vartheta) c_j^\dagger \hat{R}^{-1}(\vartheta) = \sum_{ji} D_{jk}^* R_{ij}(\vartheta) c_i^\dagger, \end{aligned} \quad (\text{A6})$$

where  $R_{ij}(\vartheta) = \langle i|\hat{R}(\vartheta)|j\rangle$  is an element of the matrix representation of the rotation operator in the single-particle basis.

Using Eq. A5, overlap and Hamiltonian matrix elements between symmetry-projected configurations are expressed in terms of norm and Hamiltonian overlaps between rotated determinants  $\hat{R}(\vartheta)|\Phi\rangle$  as

$$\langle\Phi^r|\hat{P}_{kk'}^j|\Phi^s\rangle = \frac{1}{V} \int_V d\vartheta w_{kk'}^j(\vartheta) n^{rs}(\vartheta), \quad (\text{A7a})$$

$$\langle\Phi^r|\hat{H} \hat{P}_{kk'}^j|\Phi^s\rangle = \frac{1}{V} \int_V d\vartheta w_{kk'}^j(\vartheta) n^{rs}(\vartheta) h^{rs}(\vartheta), \quad (\text{A7b})$$

where

$$n^{rs}(\vartheta) \equiv \langle\Phi^r|\hat{R}(\vartheta)|\Phi^s\rangle, \quad (\text{A8a})$$

$$h^{rs}(\vartheta) \equiv \frac{\langle\Phi^r|\hat{H} \hat{R}(\vartheta)|\Phi^s\rangle}{\langle\Phi^r|\hat{R}(\vartheta)|\Phi^s\rangle}. \quad (\text{A8b})$$

The norm overlaps of Eq. A8a can be evaluated by applying Wick's theorem on the bare fermion vacuum. This leads to

$$n^{rs}(\vartheta) = \det_N X^{rs}(\vartheta), \quad (\text{A9})$$

$$X^{rs}(\vartheta) = D^{r\top} R(\vartheta) D^{s*}. \quad (\text{A10})$$

Here,  $D^k$  is the (rectangular) matrix of occupied orbital coefficients associated with the determinant  $|\Phi^k\rangle$  and  $R(\vartheta)$  is the matrix representation of the rotation operator in the single-particle basis. The notation  $\det_N$  is used to emphasize that the determinant should be evaluated over the  $N \times N$  block of  $X^{rs}(\vartheta)$  defined by the occupied states in  $|\Phi^r\rangle$  and  $|\Phi^s\rangle$ .

The Hamiltonian overlaps of Eq. A8b can be evaluated by using an extended Wick's theorem [54] when  $|\Phi^r\rangle$  and  $|\Phi^s\rangle$  are not orthogonal. They are given by

$$h^{rs}(\vartheta) = \sum_{ik} \left[ \langle i|\hat{h}|k\rangle + \frac{1}{2} \Gamma_{ik}^{rs}(\vartheta) \right] \rho_{ki}^{rs}(\vartheta), \quad (\text{A11})$$

$$\Gamma_{ik}^{rs}(\vartheta) = \sum_{jl} \langle ij|\hat{v}|kl\rangle \rho_{lj}^{rs}(\vartheta). \quad (\text{A12})$$

The Hamiltonian overlaps are expressed in terms of the transition density matrix  $\rho^{rs}(\vartheta)$ , with elements defined by

$$\rho_{ki}^{rs}(\vartheta) \equiv \frac{\langle\Phi^r|c_i^\dagger c_k \hat{R}(\vartheta)|\Phi^s\rangle}{\langle\Phi^r|\hat{R}(\vartheta)|\Phi^s\rangle}. \quad (\text{A13})$$

The transition density matrix of Eq. A13 is built according to [53]

$$\rho^{rs}(\vartheta) = R(\vartheta) D^{s*} [X^{rs}(\vartheta)]^{-1} D^{r\top}. \quad (\text{A14})$$

Here, the inverse of  $X^{rs}(\vartheta)$  (defined in Eq. A10) should be evaluated over the  $N \times N$  block of occupied states in both determinants. Accordingly, only the occupied orbitals in  $D^r$  and  $D^s$  should be used in computing the matrix product above.

Matrix elements appearing in contributions to the energy gradient can also be expressed in terms of overlaps between rotated determinants:

$$\langle \Phi^r | b_h^{r\dagger} b_p^r \hat{P}_{kk'}^j | \Phi^s \rangle = \frac{1}{V} \int_V d\vartheta w_{kk'}^j(\vartheta) n^{rs}(\vartheta) N_{ph}^{rs}(\vartheta), \quad (\text{A15a})$$

$$\langle \Phi^r | b_h^{r\dagger} b_p^r \hat{H} \hat{P}_{kk'}^j | \Phi^s \rangle = \frac{1}{V} \int_V d\vartheta w_{kk'}^j(\vartheta) n^{rs}(\vartheta) H_{ph}^{rs}(\vartheta), \quad (\text{A15b})$$

where we have appended a superscript to the HF operators to label the determinant to which they are associated. Here,

$$N_{ph}^{rs}(\vartheta) \equiv \frac{\langle \Phi^r | b_h^{r\dagger} b_p^r \hat{R}(\vartheta) | \Phi^s \rangle}{\langle \Phi^r | \hat{R}(\vartheta) | \Phi^s \rangle}, \quad (\text{A16a})$$

$$H_{ph}^{rs}(\vartheta) \equiv \frac{\langle \Phi^r | b_h^{r\dagger} b_p^r \hat{H} \hat{R}(\vartheta) | \Phi^s \rangle}{\langle \Phi^r | \hat{R}(\vartheta) | \Phi^s \rangle}. \quad (\text{A16b})$$

The matrix elements of Eq. A16 can be evaluated using an extended Wick's theorem when  $|\Phi^r\rangle$  and  $|\Phi^s\rangle$  are not orthogonal. They are given by

$$N_{ph}^{rs}(\vartheta) = \left[ D^{r\text{T}} \rho^{rs}(\vartheta) D^{r*} \right]_{ph}, \quad (\text{A17a})$$

$$\begin{aligned} H_{ph}^{rs}(\vartheta) &= h^{rs}(\vartheta) \left[ D^{r\text{T}} \rho^{rs}(\vartheta) D^{r*} \right]_{ph} \\ &+ \left[ D^{r\text{T}} (\mathbf{1} - \rho^{rs}(\vartheta)) f^{rs}(\vartheta) \rho^{rs}(\vartheta) D^{r*} \right]_{ph}, \end{aligned} \quad (\text{A17b})$$

where we have set  $f_{ik}^{rs}(\vartheta) = \langle i | \hat{h} | k \rangle + \Gamma_{ik}^{rs}(\vartheta)$ .

- 
- [1] A. Dreuw and M. Head-Gordon, Chem. Rev. **105**, 4009 (2005).
  - [2] H.-J. Werner and W. Meyer, J. Chem. Phys. **74**, 5794 (1981).
  - [3] B. O. Roos, K. Andersson, M. P. Fulscher, P. Å. Malmqvist, L. Serrano-Andres, K. Pierloot, and M. Merchan, in *Advances in Chemical Physics: New Methods in Computational Quantum Mechanics*, Vol. 93, edited by I. Prigogine and S. A. Rice (Wiley, New York, 1996) pp. 219–231.
  - [4] A. I. Krylov, Annu. Rev. Phys. Chem. **59**, 433 (2008).
  - [5] J. D. Watts, in *Radiation Induced Molecular Phenomena in Nucleic Acids: A Comprehensive Theoretical and Experimental Analysis*, edited by M. K. Shukla and J. Leszczynski (Springer, 2008) pp. 65–92.

- [6] X. Li and J. Paldus, J. Chem. Phys. **134**, 214118 (2011).
- [7] V. V. Ivanov, D. I. Lyakh, and L. Adamowicz, Annu. Rep. Prog. Chem., Sect. C: Phys. Chem. **107**, 169 (2011).
- [8] H. Nakatsuji, Chem. Phys. Lett. **67**, 329 (1979).
- [9] M. Rohlfing, Int. J. Quantum Chem. **80**, 807 (2000).
- [10] T. Kuś, V. F. Lotrich, and R. J. Bartlett, J. Chem. Phys. **130**, 124122 (2009).
- [11] M. E. Casida and M. Huix-Rotllant, Annu. Rev. Phys. Chem. **63**, 287 (2012).
- [12] J. B. Foresman, M. Head-Gordon, J. A. Pople, and M. J. Frisch, J. Phys. Chem. **96**, 135 (1992).
- [13] K. W. Schmid, F. Grümmer, M. Kyotoku, and A. Faessler, Nucl. Phys. A **452**, 493 (1986).
- [14] K. W. Schmid, Prog. Part. Nucl. Phys. **52**, 565 (2004).
- [15] R. Rodríguez-Guzmán, K. W. Schmid, C. A. Jiménez-Hoyos, and G. E. Scuseria, Phys. Rev. B, 245130 (2012).
- [16] R. Rodríguez-Guzmán, C. A. Jiménez-Hoyos, R. Schutski, and G. E. Scuseria, Phys. Rev. B **87**, 235129 (2013).
- [17] P.-O. Löwdin, Phys. Rev. **97**, 1509 (1955).
- [18] P.-O. Löwdin, in *Quantum Theory of Atoms, Molecules, and the Solid State: A Tribute to John C. Slater*, edited by P.-O. Löwdin (Academic Press, New York, 1966) pp. 601–623.
- [19] C. A. Jiménez-Hoyos, T. M. Henderson, T. Tsuchimochi, and G. E. Scuseria, J. Chem. Phys. **136**, 164109 (2012).
- [20] B. F. Bayman, Nucl. Phys. **15**, 33 (1960).
- [21] F. Villars, in *Varennia Lectures*, Vol. 36, edited by C. Bloch (Academic Press, New York, 1966) p. 1.
- [22] J. K. Percus and A. Rotenberg, J. Math. Phys. **3**, 928 (1962).
- [23] P. Ring and P. Schuck, *The Nuclear Many-Body Problem* (Springer-Verlag, Berlin, 1980).
- [24] Here,  $\hat{P}$  may stand for a product of projection operators for say, spin and point group restoration.
- [25] K. W. Schmid, F. Grümmer, and A. Faessler, Phys. Rev. C **29**, 291 (1984).
- [26] H. B. Schlegel, J. Chem. Phys. **84**, 4530 (1986).
- [27] I. Mayer, Adv. Quantum Chem. **12**, 189 (1980).
- [28] H. J. Mang, Phys. Rep. **18**, 325 (1975).
- [29] J. Noga and J. Šimunek, J. Chem. Theory Comput. **6**, 2706 (2010).
- [30] G. B. Backsay, Chem. Phys. **61**, 385 (1981).
- [31] J. L. Egido, J. Lessing, V. Martin, and L. M. Robledo, Nucl. Phys. A **594**, 70 (1995).
- [32] C. A. Jiménez-Hoyos, *Variational approaches to the molecular electronic structure problem based on symmetry-projected Hartree–Fock configurations*, Ph.D. thesis, Rice University (2013).
- [33] C. A. Jiménez-Hoyos, R. Rodríguez-Guzmán, and G. E. Scuseria, Phys. Rev. A **86**, 052102 (2012).
- [34] J. Nocedal and S. J. Wright, *Numerical Optimization*, 2nd ed., Springer Series in Operations Research and Financial Engineering (Springer, New York, 2006).
- [35] C. A. Jiménez-Hoyos, R. Rodríguez-Guzmán, and G. E. Scuseria, J. Chem. Phys. (2013), submitted.

- [36] H. Fukutome, Prog. Theor. Phys. **80**, 417 (1988).
- [37] K. W. Schmid, Z. Ren-Rong, F. Grümmner, and A. Faessler, Nucl. Phys. A **499**, 63 (1989).
- [38] H. Koch and E. Dalggaard, Chem. Phys. Lett. **212**, 193 (1993).
- [39] J. Nocedal, Math. Comput. **35**, 773 (1980).
- [40] D. C. Liu and J. Nocedal, Math. Program. **45**, 503 (1989).
- [41] M. J. Frisch, G. W. Trucks, H. B. Schlegel, G. E. Scuseria, M. A. Robb, J. R. Cheeseman, G. Scalmani, V. Barone, B. Mennucci, G. A. Petersson, H. Nakatsuji, M. Caricato, X. Li, H. P. Hratchian, A. F. Izmaylov, J. Bloino, G. Zheng, J. L. Sonnenberg, M. Hada, M. Ehara, K. Toyota, R. Fukuda, J. Hasegawa, M. Ishida, T. Nakajima, Y. Honda, O. Kitao, H. Nakai, T. Vreven, J. A. Montgomery, Jr., J. E. Peralta, F. Ogliaro, M. Bearpark, J. J. Heyd, E. Brothers, K. N. Kudin, V. N. Staroverov, R. Kobayashi, J. Normand, K. Raghavachari, A. Rendell, J. C. Burant, S. S. Iyengar, J. Tomasi, M. Cossi, N. Rega, J. M. Millam, M. Klene, J. E. Knox, J. B. Cross, V. Bakken, C. Adamo, J. Jaramillo, R. Gomperts, R. E. Stratmann, O. Yazyev, A. J. Austin, R. Cammi, C. Pomelli, J. W. Ochterski, R. L. Martin, K. Morokuma, V. G. Zakrzewski, G. A. Voth, P. Salvador, J. J. Dannenberg, S. Dapprich, A. D. Daniels, . Farkas, J. B. Foresman, J. V. Ortiz, J. Cioslowski, and D. J. Fox, Gaussian Development Version, Revision H.1, Gaussian Inc., Wallingford, CT, 2009.
- [42] M. L. Abrams and C. D. Sherrill, J. Chem. Phys. **121**, 9211 (2004).
- [43] C. D. Sherrill and P. Piecuch, J. Chem. Phys. **122**, 124104 (2005).
- [44] M. B. Robin, *Higher Excited States of Polyatomic Molecules*, Vol. 3 (Academic Press, New York, 1985).
- [45] S. Taylor, D. G. Wilden, and J. Comer, Chem. Phys. **70**, 291 (1982).
- [46] C. M. Hadad, J. B. Foresman, and K. B. Wiberg, J. Phys. Chem. **97**, 4293 (1993).
- [47] J. Pitarch-Ruiz, J. Sánchez-Marín, A. Sánchez de Meras, and D. Maynau, Mol. Phys. **101**, 483 (2003).
- [48] M. Schreiber, M. R. Silva-Junior, S. P. A. Sauber, and W. Thiel, J. Chem. Phys. **128**, 134110 (2008).
- [49] This, however, does not imply that all the triplet components in a symmetry-projected construction are not degenerate. If a UHF-type determinant  $|\Phi\rangle$  has  $m_s = z$ , then all  $2j + 1$  states of the form  $\hat{P}_{mz}^j |\Phi\rangle$ , with  $m = -j, \dots, +j$ , are degenerate.
- [50] J.-P. Daudey, J.-L. Heully, and J.-P. Malrieu, J. Chem. Phys. **99**, 1240 (1993).
- [51] G. D. Purvis, III, R. Shepard, F. B. Brown, and R. J. Bartlett, Int. J. Quantum Chem. **23**, 835 (1983).
- [52] F. A. Evangelista, W. D. Allen, and H. F. Schaefer, III, J. Chem. Phys. **125**, 154113 (2006).
- [53] P.-O. Löwdin, Phys. Rev. **97**, 1490 (1955).
- [54] J.-P. Blaizot and G. Ripka, *Quantum Theory of Finite Systems* (The MIT Press, Cambridge, MA, 1985).